Evolving a $10^6\,M_\odot$ star along the Hayashi track: Exploring the mass-radius relation of a proto globular cluster cloud

Anna Sippel (Swinburne University)
Supervised by Norman Murray (CITA)

September 16, 2014

Abstract

We explore the mass-radius relation of a proto globular cluster cloud. This is motivated by the finding that observed clusters in the mass range $10^4 - 10^6\,M_\odot$ show no systematic variation of radius with mass, while clusters with masses larger than $3 \times 10^6\,M_\odot$ have an increasing size with increasing mass. Murray (2009) show that those massive clusters were optically thick to far-infrared radiation when they formed, leading for the size of them set by a balance between radiation pressure (powered by accretion) and gravity. We aim to create a model of such a proto cluster cloud (before its fragmentation) to investigate this theory, and use `MESA` to do so.

1 Introduction: Globular cluster systems

Globular clusters (GCs) are the most massive of all star clusters (SCs), with generally at least 100 000 member stars, and are fundamental components of galaxies. Galaxies host two subpopulations of GCs, one appearing blue, and the other appearing red (Zinn, 1985; Ashman & Zepf, 1992; Zepf & Ashman, 1993). The red clusters are more centrally concentrated than the blue ones within the host galaxy, with the red clusters located predominantly in the bluge and the blue ones in the halo (Brodie & Strader, 2006). Both, blue and red clusters are old with ages $> 10\,\mathrm{Gyr}$ (Milone et al., 2012). The bimodality is driven by a difference in metallicity, with the red clusters being metal-rich and the blue clusters metal-poor, as confirmed spectroscopically (Usher et al. 2012 and references therein).

Average properties of GC populations are found to correlate with fundamental characteristics of their host galaxy. More luminous galaxies tend to feature larger GC populations (Brodie & Strader, 2006), of up to several thousands, in the case of giant elliptical galaxies (Peng et al., 2011), in contrast to ~ 160 currently known in the Milky Way (MW; Harris 2010) at distances up to $\sim 145\,\mathrm{kpc}$ from the Galactic center (Laevens et al., 2014). The mass of the GC system of a galaxy has been shown to correlate with galaxy halo mass (Spitler & Forbes, 2009; Hudson et al., 2014), independent of galaxy morphology (Georgiev et al., 2010) and a connection between the number of GCs and the mass of the central black hole of a galaxy has been found (Burkert & Tremaine, 2010; Harris & Harris, 2011). Maschberger & Kroupa (2007) presented a method to derive the star formation history of a galaxy by its GC distribution under the assumption that all stars form in SCs, with GCs representing the high-mass end of the SC mass function. Muratov & Gnedin (2010) estimate that at redshifts $z > 3$ more than 10% of

the galactic stellar mass was locked in GCs compared to just 0.1% now, and that more than 20% of the star formation (SF) in galaxies at $z > 3$ took place in GCs.

While it is nowadays widely accepted that the majority of stars form in clusters (Lada & Lada, 1995; Allen et al., 2007), the formation of SCs and in particular GCs is only poorly understood. Depending on their age, SCs are either well preserved remnants of the first era of SF in a galaxy or tracers of major SF events induced by, for example, mergers (Brodie & Strader, 2006; Renaud et al., 2011). Similarly, while we observe GCs in very different environments in and around their host galaxies (i.e. bulge or halo), their origin (i.e. in-situ or external) is not very well constrained (Brodie & Strader, 2006). Recent simulations show that the GC bimodality can naturally occur in a hierarchical galaxy assembly, with the red population formed in the main progenitor while the blue sub-population is accreted from satellites and formed earlier (Tonini, 2013). This agrees well with the recent finding that the distinction between blue and red clusters extends to their dynamical properties, with the red clusters following the rotation of the galaxy and the blue clusters the non-rotation of the halo (Pota et al., 2013).

1.1 Evolution of globular clusters

It is still computationally expensive and hence a challenge to include GCs in simulations of galaxy evolution. Within cosmological (dark-matter only) N-body simulations, the mass of one particle is usually more massive than one entire GCs. Re-simulation techniques (e.g. Martig et al. 2009, 2012) including gas and stars have a spatial resolution of 150 pc and particle masses of $1.5 \times 10^4\,M_\odot$ for gas, $7.5 \times 10^4\,M_\odot$ for stars, and $3 \times 10^5\,M_\odot$ for dark matter. This implies that a two-stage process is necessary for the accurate modeling of GC evolution after formation: orbital parameters as well as the mass and shape of the host galaxy can be extracted from cosmological simulations, and in a second step this information can be used as input parameters for direct N-body simulations of star cluster evolution. This approach has been implemented by Renaud et al. (2011) and allows for a much better understanding of the origin of the young clusters in the merger of the Antennae galaxies. However, the process of the formation of the GC itself is not yet included in this approach and assumptions on the initial conditions of GCs need to be made, in particular mass and radius. While both those parameters are reasonably well determined for today's open clusters in the solar neighborhood as well as the old GCs we observe today in the Milky Way and nearby galaxies – their initial conditions are not.

The lifetime of a GC depends on those parameters (as well as the external tidal field), and can be divided in two main stages:

- The first $\leqslant 2$ Gyr are dominated by stellar evolution driven expansion, and depending on metallicity, stars with masses $\geqslant 2\,M_\odot$ will end their life within this time and do so accompanied by heavy mass loss. The cluster reacts to this mass loss with an increase in size.

- After this time, the mass loss is dominated by the continued but slower loss of stars from the cluster. Stars can be ejected via few-body encounters, they can receive a velocity kick during a supernova explosion, or they can simply pass beyond the tidal boundary of the cluster. This is particularly effective close to the disk of the external potential, noting that disk crossings occur at a frequency of the order of ~ 100 Myr for inclined orbits at galactocentric distances comparable to the Sun. Simultaneously, stellar encounters are

so common that they sort the distribution of stars over time: low-mass stars increase their velocity and travel towards the outskirts of the cluster, while high-mass stars sink to the bottom of the potential well. This process, following a trend towards equipartition of energies, is called mass segregation.

The combination of those processes implies that the GCs we observe today are only the remnants of a cluster that originally formed. The mass and size of clusters (Madrid et al., 2012), distribution of stars (Baumgardt et al., 2008) and the mass function (Baumgardt & Makino, 2003; Lamers et al., 2006) change over time, making it difficult to reconstruct the clusters initial conditions. However some remarkable trends remain:

- *On average*, all GCs have similar half-light radii of $\sim 3\,\mathrm{pc}$ (or 2.66 pc in the Virgo cluster, see Jordán et al. 2005). This holds true for a range of masses, matallicities, host galaxy and environment and possibly initial mass function and age.

- Similarly, the mass-radius relation for GCs is uniform over a wide range of masses (see Fig. 1). In particular, clusters with $M \gtrsim 10^6\,M_\odot$ are unaffected by stellar evolution, while clusters with $M \gtrsim 10^5 M_\odot \times (4\,\mathrm{kpc}/\mathrm{R_G})$ are not affected by the tidal field (Gieles et al., 2010, 2011).

This accumulates in Fig. 1 (which is extracted from Gieles et al. 2010), where the mass-radius relation is shown for various hot stellar systems (open cluster, GCs, massive GCs, ultra compact dwarf galaxies and dwarf-GC transition objects). It can be seen that the mass-radius relation can be divided into two regimes: The high-mass end of clusters unaffected by both stellar evolution and the tidal field, and a lower mass end affected by stellar evolution, with the break occurring at roughly $10^4\,M_\odot$. The mass-radius relation of observed clusters is also compared to the Faber-Jackson relation Faber & Jackson (1976), however corrected for stellar evolution. The agreement is remarkable given the different nature of star clusters and elliptical galaxies, for which the relation $L \propto \sigma^\gamma$ was derived. Here, σ is the velocity dispersion and $\gamma \approx 4$.

A similar figure was also presented in Murray (2009), including a wider range of masses in the mass-radius relation reaching down to embedded young clusters. The this allows for three regimes to be visible in the mass-radius relation: $M \gtrsim 10^6\,M\odot$ and $10^4\,M_\odot \leq M \leq 10^6\,M_\odot$ and also $M < 10^4\,M_\odot$. The low-mass clusters again follow a similar slope as the high mass ones, not yet affected by the list of destruction mechanisms given above. On the other hand the clusters with high enough masses $\gtrsim 3 \times 10^6\,M_\odot$ still follow their *initial* mass-radius relation.

Most recently, a similar figure has been published by Norris et al. (2014), and a so-called *zone of avoidance* (see Fig. 3) similar to the forbidden zone to the right of the Hayashi track is defined. The zone of avoidance is a by-eye fit to the mass-radius relation of elliptical galaxies, dwarf ellipticals and compact ellipticals as determined by Misgeld & Hilker (2011).

It is the aim of this project to better determine the physical origin of such a *zone of avoidance* for GCs.

2 The physics of the pre-cluster cloud

2.1 Sun-like proto stars

Pre-main sequence stars (PMSs) of a mass comparable to the Sun obey a luminosity-temperature relation, which manifests itself in an almost vertical line in the Hertzsprung-Russel diagram.

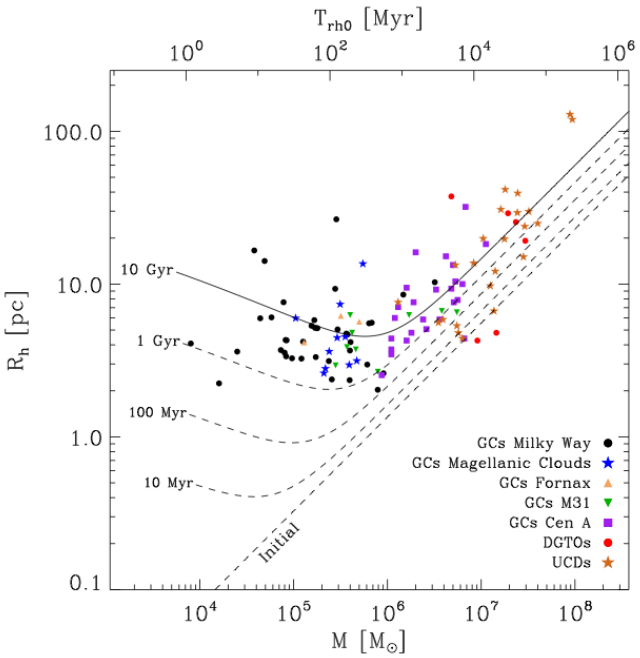

Figure 1: Mass-radius values for hot stellar systems (figure adapted from Gieles et al. 2010). The lines show the evolution of the mass-radius relation using the Faber-Jackson relation, corrected for stellar evolution, as initial conditions. The break at $\sim 10^6\,M_\odot$ at $T \approx 10\,\mathrm{Gyr}$ is because lower mass objects have expanded

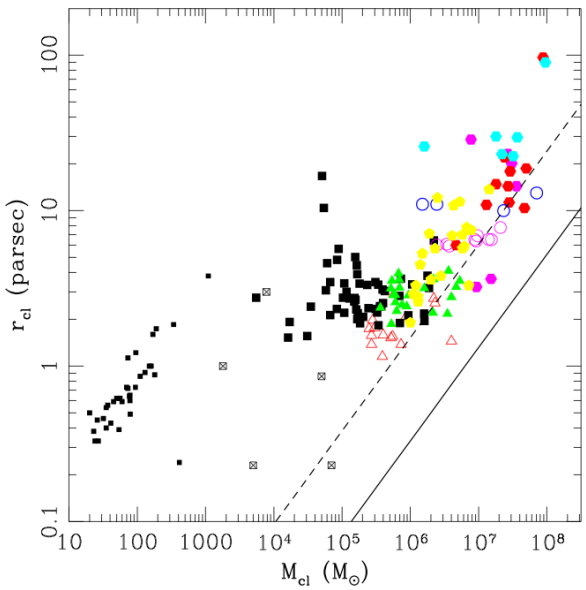

Figure 2: Mass-radius values for hot stellar systems (figure adapted from Murray 2009). The solid line is the relation given in Equation 3 (and as derived in Eq. 17 from Murray 2009), while the dashed line is the same but corrected for stellar evolution.

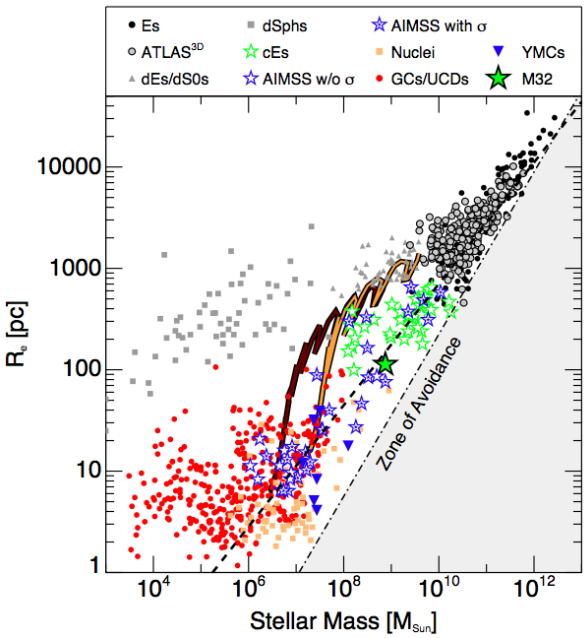

Figure 3: Mass-radius relation for compact stellar systems (figure adapted from Norris et al. (2014)). The *zone of avoidance* is defined by Misgeld & Hilker (2011).

The cloud is no longer in free-fall, but still shrinking (which will continue as long as the inward force is larger than the radiation pressure). It moves along the Hayashi boundary (Hayashi, 1961) with slowed contraction and decreasing luminosity L following

$$L = 4\pi R^2 \sigma T_{\rm eff}^4 \tag{1}$$

where R is the stars radius, $T_{\rm eff}$ the effective temperature and σ the Stefan-Boltzmann constant. A schematic overview is given in Fig. 4, and no star in hydrostatic equilibrium can be in the *forbidden* zone. A Sun-like star leaves the Hayashi track when contraction is halted. This occurs with the ignition of nuclear fusion (i.e. entering the main sequence).

2.2 Massive clouds $> 3 \times 10^6\,{\rm M}_\odot$

Murray (2009) argues that the change of the slope in the mass-radius relation around $10^6\,M_\odot$ occurs due to the emergence of radiation pressure in the proto-cluster cloud. In general, there are three possible states Today's clusters in the Milky way are optically thin to far-infrared radiation (FIR), implying that the temperature is independent of cluster radius or density. If however he proto cluster is optically thick to FIR, the gas temperature will be higher, leading to a higher Jeans mass. If the cloud has a FIR optical depth $\tau > 1$ and is massive enough, the accretion luminosity $L_{\rm acc}$ becomes dynamically important. As long as the outward force caused by the radiation $F = \tau L_{\rm acc}/c$ is less than the counteracting force due to gravity, the cloud continues to shrink. The accretion luminosity of a cluster contracting at the free-fall time $t_{ff} = \sqrt{3\pi/32G\rho}$ is

$$L_{\rm acc} = \frac{GM_{\rm cl}^2}{r_{\rm cl} t_{ff}} \propto v^5/G \tag{2}$$

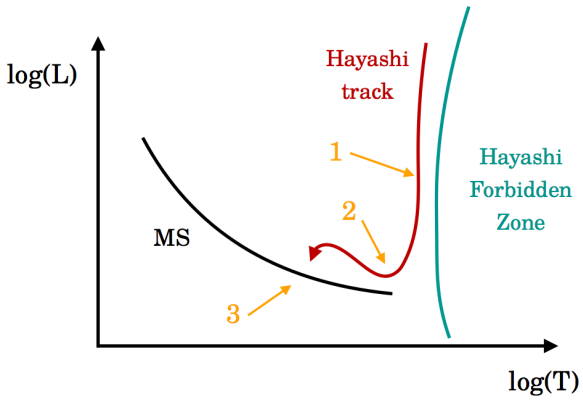

Figure 4: Schematic overview of the Hayashi track: Before entering the main sequence, a fully convective proto-star descents on the Hayashi track (1), develops a radiative core (2)and commences hydrogen burning when entering the main sequence (3, MS).

with G the gravitational constant and $v = \sqrt{GM_{\rm cl}/r_{\rm cl}}$. $M_{\rm cl}$ and $r_{\rm cl}$ are the clouds mass and radius. Hence $L_{\rm acc} \sim r^{-5/2}$ and to first order, the optical depth goes as $\tau \sim r_{\rm cl}^{-2}$ (Eq. 9-13 in Murray 2009). This implies that the outward force caused by radiation increases as $F_{\rm rad} \sim r^{-9/2}$, while the force of gravity of course increases as $F_{\rm grav} \sim r^{-2}$. Hence for small enough radii $r_{\rm rad}$ the collapse is slowed from the free-fall to the Kelvin rate, and this occurs at

$$r_{\rm rad} \sim G^{1/5} \left(\frac{\kappa}{4\pi c}\right)^{2/5} M_{\rm cl}^{3/5} \tag{3}$$

(see Eq. 17 and Appendix C of Murray 2009).

In summary, $\mathbf{r_{rad} \sim M_{cl}^{3/5}}$. Can we reproduce this, modelling a collapsing gas cloud? If so, is this equivalent to the Hayashi track for Sun-like stars? If so, this will enable us to constrain the *maximum density* at which a GC can form.

3 Approach: MESA

We use `MESA`[1] for this project. This code is a state-of-the-art, modular, open source software for stellar evolution from pre-main sequence until the remnant phase (Paxton et al., 2011, 2013). Models are evolved by using a standard library and a list of specific input parameters. The evolution of the models can be monitored via real-time output.

Previously, I had never used `MESA`. The code is designed to evolve *stars* up to no more than $\sim 1000\,M_\odot$, implying we want to use the `MESA` framework, but test if we can take it way beyond its intentions. `MESA` is well documented, but the huge amount of options available make it not straight forward to get it running as desired.

As a first step I got familiar with the code and evolved some Sun-like as well as more massive stars to test the environment and parameters. I also wrote several plotting scripts to extract the output and turn it into movies when desired, some examples are given in Fig. 5 & 6.

[1]Modules for Experiments in Stellar Astrophysics: `mesa.sourceforge.net/index.html`

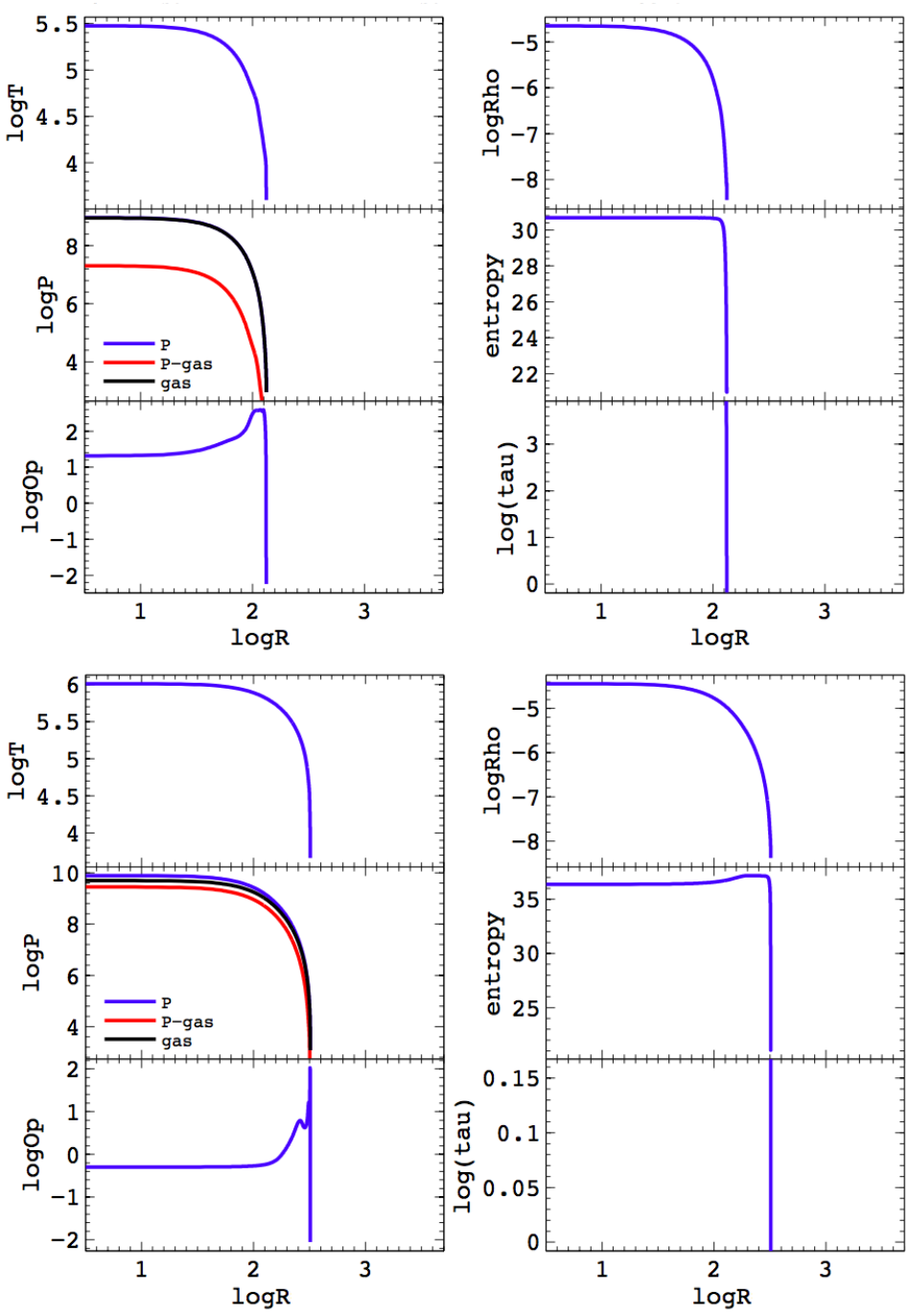

Figure 5: Visualization of several radial parameters for a star of 5 $M_\odot$ (top panels) and 60 $M_\odot$ (bottom panels) at the beginning of the model.

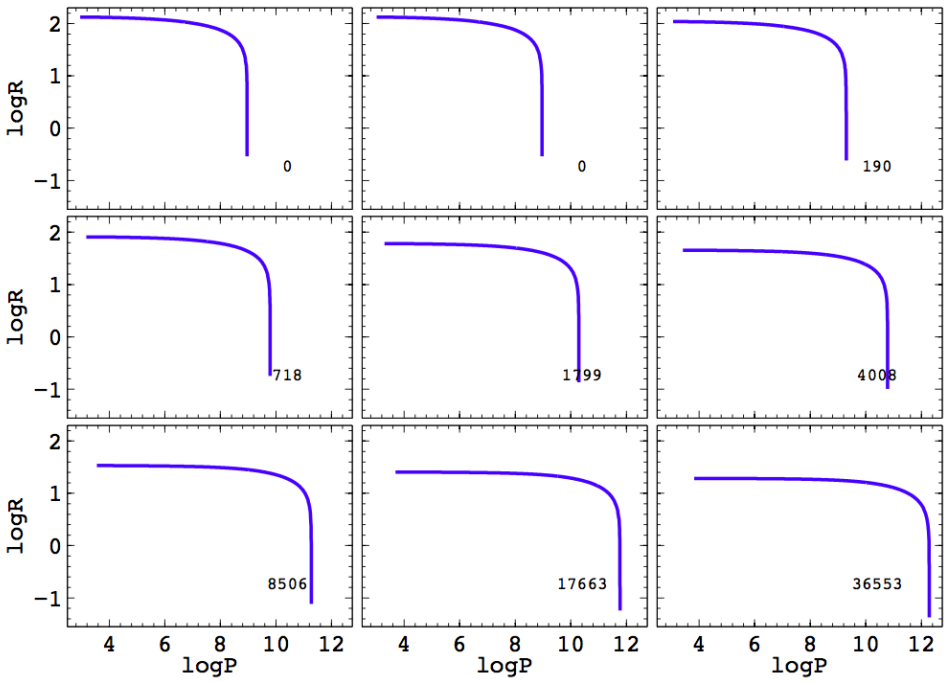

Figure 6: Time evolution of the pressure-radius relation between zero and 36553 Myr.

4 Outlook

MESA allows parameters such as mass, temperature or density to be set from an input file. The parameters are adjusted step by step by solving the equation of state from pre-existing models. In practice, this means that we begin a model by using a $30\,M_\odot$ cloud and add mass on top of it, step by step. This process only works up to a few thousand solar masses, but at higher temperatures than we prefer for a proto-cluster cloud. In other words, nuclear fusion is ignited in the center of the cloud, which is not the desired outcome. In addition, this process is rather time (and space) consuming on a laptop.

Now that I have become more familiar with MESA, I have a running installation on the Supercomputer at Swinburne, allowing me to run more, more sophisticated and longer models. The next steps will be to take a different approach to build the starting model: instead of letting MESA add the mass to the cloud, we will iterate the evolution between MESA and external codes to build the starting model step by step with more control. This approach has been used by James Owen at CITA to create stars less massive than automatically supported my MESA.

The enhanced understanding of GC formation from this project will significantly help us in understanding the physics of the physics of the pre-cluster cloud and hence in constraining the initial conditions of GCs (in particular the density). This on the other hand will improve the initial conditions used for direct N-body models of GCs and help us understand more about the mass-to-light ratios and initial mass functions of GCs.

5 Acknowledgments

I thank Pascale Garaud for organizing the ISIMA workshop and Norman Murray for the idea of this project and his time and support. This project and report are based on his earlier work *The sizes and luminosities of massive star clusters* (Murray, 2009). Though the project is not yet finished, it will be continued in the coming months. I am grateful for the opportunity of this excursion into a field which I was previously completely unfamiliar with.

References

Allen L., Megeath S. T., Gutermuth R., Myers P. C., Wolk S., Adams F. C., Muzerolle J., Young E., Pipher J. L., 2007, Protostars and Planets V, 361

Ashman K. M., Zepf S. E., 1992, ApJ, 384, 50

Baumgardt H., De Marchi G., Kroupa P., 2008, ApJ, 685, 247

Baumgardt H., Makino J., 2003, MNRAS, 340, 227

Brodie J. P., Strader J., 2006, ARA&A, 44, 193

Burkert A., Tremaine S., 2010, ApJ, 720, 516

Faber S. M., Jackson R. E., 1976, ApJ, 204, 668

Georgiev I. Y., Puzia T. H., Goudfrooij P., Hilker M., 2010, MNRAS, 406, 1967

Gieles M., Baumgardt H., Heggie D. C., Lamers H. J. G. L. M., 2010, MNRAS, 408, L16

Gieles M., Heggie D. C., Zhao H., 2011, MNRAS, 413, 2509

Harris G. L. H., Harris W. E., 2011, MNRAS, 410, 2347

Harris W. E., 2010, arXiv:1012:3224

Hayashi C., 1961, Publ. Astron. Soc. Japan, 13, 450

Hudson M. J., Harris G. L., Harris W. E., 2014, ApJ, 787, L5

Jordán A., Côté P., Blakeslee J. P., Ferrarese L., McLaughlin D. E., Mei S., Peng E. W., Tonry J. L., Merritt D., Milosavljević M., Sarazin C. L., Sivakoff G. R., West M. J., 2005, ApJ, 634, 1002

Lada E. A., Lada C. J., 1995, AJ, 109, 1682

Laevens B. P. M., Martin N. F., Sesar B., Bernard E. J., Rix H.-W., Slater C. T., Bell E. F., Ferguson A. M. N., Schlafly E. F., Burgett W. S., Chambers K. C., Denneau L., Draper P. W., Kaiser N., Kudritzki R.-P., Magnier E. A., Metcalfe N., Morgan J. S., Price P. A., Sweeney W. E., Tonry J. L., Wainscoat R. J., Waters C., 2014, ApJ, 786, L3

Lamers H. J. G. L. M., Anders P., de Grijs R., 2006, A&A, 452, 131

Madrid J. P., Hurley J. R., Sippel A. C., 2012, ApJ, 756, 167

Martig M., Bournaud F., Croton D. J., Dekel A., Teyssier R., 2012, ApJ, 756, 26

Martig M., Bournaud F., Teyssier R., Dekel A., 2009, ApJ, 707, 250

Maschberger T., Kroupa P., 2007, MNRAS, 379, 34

Milone A. P., Piotto G., Bedin L. R., Aparicio A., Anderson J., Sarajedini A., Marino A. F., Moretti A., Davies M. B., Chaboyer B., Dotter A., Hempel M., Marin-Franch A., Majewski S., Paust N. E. Q., Reid I. N., Rosenberg A., Siegel M., 2012, A&A, 540, A16

Misgeld I., Hilker M., 2011, MNRAS, 414, 3699

Muratov A. L., Gnedin O. Y., 2010, ApJ, 718, 1266

Murray N., 2009, ApJ, 691, 946

Norris M. A., Kannappan S. J., Forbes D. A., Romanowsky A. J., Brodie J. P., Faifer F. R., Huxor A., Maraston C., Moffett A. J., Penny S. J., Pota V., Smith-Castelli A., Strader J., Bradley D., Eckert K. D., Fohring D., McBride J., Stark D. V., Vaduvescu O., 2014, MNRAS, 443, 1151

Paxton B., Bildsten L., Dotter A., Herwig F., Lesaffre P., Timmes F., 2011, ApJS, 192, 3

Paxton B., Cantiello M., Arras P., Bildsten L., Brown E. F., Dotter A., Mankovich

C., Montgomery M. H., Stello D., Timmes F. X., Townsend R., 2013, ApJS, 208, 4
Peng E. W., Ferguson H. C., Goudfrooij P., 2011, ApJ, 730, 23
Pota V., Forbes D. A., Romanowsky A. J., Brodie J. P., Spitler L. R., Strader J., Foster C., Arnold J. A., Benson A., Blom C., Hargis J. R., Rhode K. L., Usher C., 2013, MNRAS, 428, 389
Renaud F., Gieles M., Boily C. M., 2011, MNRAS, 418, 759
Spitler L. R., Forbes D. A., 2009, MNRAS, 392, L1
Tonini C., 2013, ApJ, 762, 39
Usher C., Forbes D. A., Brodie J. P., Foster C., Spitler L. R., Arnold J. A., Romanowsky A. J., Strader J., Pota V., 2012, MNRAS, 426, 1475
Zepf S. E., Ashman K. M., 1993, MNRAS, 264, 611
Zinn R., 1985, ApJ, 293, 424